Available online at www.sciencedirect.com
SCIENCE DIRECT
Applied Catalysis A: General 302 (2006) 14–21
APPLIED CATALYSIS A: GENERAL
www.elsevier.com/locate/apcata

Low temperature water-gas shift: Type and loading of metal impacts decomposition and hydrogen exchange rates of pseudo-stabilized formate over metal/ceria catalysts

Gary Jacobs, Sandrine Ricote, Burtron H. Davis *

Center for Applied Energy Research, University of Kentucky, 2540 Research Park Drive, Lexington, KY 40511, USA

Received 13 July 2005; received in revised form 26 October 2005; accepted 29 October 2005
Available online 7 February 2006

Abstract

In this investigation, a similar degree of surface shell reduction among a series of metal promoted ceria catalysts was established by diffuse reflectance Fourier transform infrared spectroscopy (DRIFTS) and X-ray absorption near-edge spectroscopy (XANES) measurements. Surface formate species were generated by reaction of CO with bridging OH groups associated with the Ce^{3+} defect sites. The thermal decomposition of the pseudo-stable formates was followed in the absence of H_2O. Decomposition and exchange from H to D of the pseudo-stabilized formate was enhanced by changing the promoter from Au to Pt. Likewise, an increase was observed in both decomposition and exchange rates by increasing the promoter loading from 0.5 to 2.5 wt.%. The results suggest that C–H bond breaking is facilitated during this thermal decomposition (i.e., reverse decomposition to CO and –OH). Therefore, since the rate limiting step of the forward formate decomposition (i.e., the WGS reaction) is strongly suggested to be associated with C–H bond cleaving in the formate intermediate (based on earlier kinetic isotope effect and isotopic tracer studies), the results can explain the promotion in the WGS rates as observed by changing from Au to Pt and by increased promoter loading.

Keywords: Gold (Au); Platinum (Pt); Ceria (CeO_2); Formate; Water-gas shift; H–D exchange; DRIFTS

1. Introduction

The synergism between metal promoter and ceria is not well understood. Past studies have shown that a metal promoter facilitates the reduction of the ceria surface shell (e.g., [1–4]). From a formate mechanistic perspective, this is interpreted to result in enhanced Type II bridging OH group site densities at low temperature following dissociation of H_2O at surface Ce^{3+} defects (i.e., O vacancies) [3–5]. It is also important to note that bridging OH groups can also form directly, especially when a noble metal promoter like Pt is present, via dissociation and spillover of hydrogen from the metal to the oxide surface. The Type II bridging OH groups are proposed to be the OH groups, which react with CO to generate the surface formate intermediate of the water-gas shift reaction. The two proposed routes of bridging OH group formation are:

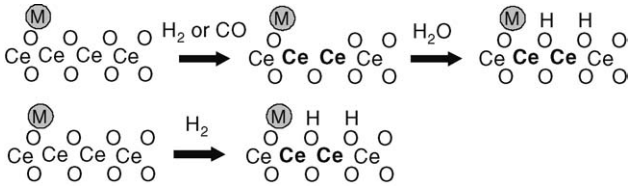

On the other hand, from the point of view of the ceria-mediated redox mechanistic perspective, O vacancy generation is an important step in the proposed catalytic cycle [6].

Yet it has been found that Au promotes the surface reduction of ceria at lower temperature than Pt [7,8], but that Pt/ceria is more active for WGS on an equivalent loading basis [8], indicating that the metallic function likely plays an additional direct role in the surface catalytic mechanism. In fact, on an equivalent loading basis, we found that 20 times as much Au/ceria was required to achieve a similar lightoff curve as Pt/ceria, even when similar extents of ceria reduction had been observed. In reviewing the history of the formate mechanism, WGS is very much related to the catalysis of formic acid decomposition. In fact, Mars et al. [9] showed that while some oxides

* Corresponding author. Tel.: +1 859 257 0253; fax: +1 859 257 0302.
E-mail address: davis@caer.uky.edu (B.H. Davis).

0926-860X/$ – see front matter © 2005 Elsevier B.V. All rights reserved.
doi:10.1016/j.apcata.2005.10.052

promote dehydrogenation of formic acid (e.g., zinc oxide, iron oxide, and chromia), other oxides are selective for the dehydration of formic acid (e.g., silica, titania). The catalysts that are active for WGS are also the same ones that are active for formic acid dehydrogenation. In considering the formate mechanism, then, one additional possibility for the role of the metal is that it may facilitate dehydrogenation of surface intermediates (e.g., surface formate during WGS or methoxy species during steam reforming of methanol).

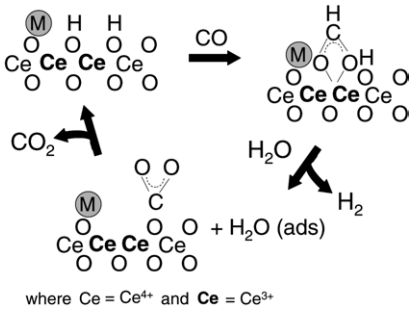

While some argue that a redox mechanism is operating [6], this is not supported by many infrared studies carried out at low temperature [4,5,10–14], including results of isotopic tracer studies for the forward shift reaction (i.e., in which H_2O was included in the feed) [14]. The argument that formates exhibit limited thermal stability [15], in our view, only enhances the likelihood that they are potentially intermediates for WGS in the low temperature regime. We find that while the formates are quite stable in the absence of H_2O (thermally decomposing in 6–8 min to reactants CO, and –OH at 300 °C), formates react very rapidly in the presence of steam, forward decomposing WGS products in 6–8 min at only 140 °C) [13]. We do not disagree, however, that at some much higher temperature, the Type II bridging OH groups will be unstable such that the mechanism could switch to a redox process. Interestingly, Binet et al. have observed Type II bridging OH groups up to 500 °C, indicating the difficulty in which chemisorbed H_2O (e.g., dissociated) is removed from the surface [16]. Type II OH groups are also observed to be active sites for WGS over thoria catalysts [17]. We continue to be intrigued by the possibility of a formate mechanism, one in which the Type II bridging OH groups promote the formation of formates via reaction with CO, and in which the forward formate decomposition is reactant promoted by H_2O [5,13]. In this contribution, we attempt to establish whether the presence of the metal promoter could also impact the rate of the formate dehydrogenation step.

In previous studies, we have demonstrated that the metal loading and type impacts the WGS rate [4]. To determine if the formate decomposition rate is impacted by the metal, we are carrying out H–D switching experiments in the presence of the pseudo-stabilized surface formate (i.e., H_2O is absent). The exchange is followed for two different metal loadings: 0.5 and 2.5% and for two different metal promoters: Au and Pt. After appropriate activation, the relative WGS rates at 250 °C have previously been observed to be 2.5% Pt > 0.5% Pt > 2.5% Au > 0.5% Au. In this study, we examine the rate of the H–D exchange to determine if the metal (both type and loading) can impact this exchange rate. If so, the implication is that the formate dehydrogenation rate will also likely be directly affected during WGS. This could therefore explain the observed wide differences in catalytic activity between Pt and Au catalysts for which equivalent extents of ceria reduction had been ascertained.

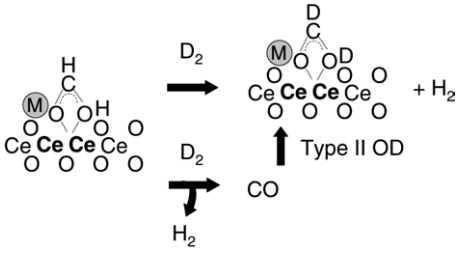

2. Experimental

2.1. Catalyst preparation

High surface area ceria was prepared by homogeneous precipitation of cerium nitrate using urea to slowly release the precipitating agent, OH^-, and the preparation procedure is reported elsewhere [4]. The ceria was dried and calcined in a muffle furnace at 400 °C for 4 h. Nano-sized gold clusters were formed utilizing the sublimation of dimethyl acetylacetonate gold under vacuum, followed by calcination at 250 °C in O_2 to decompose the ligands, and is reported previously [8]. Standard incipient wetness impregnation (IWI) was utilized to load Pt via the tetra-ammine platinum nitrate salt [4] and re-calcined at 400 °C.

2.2. BET surface area

Surface area measurements were conducted using a Micromeritics Tristar 3000 gas adsorption analyzer. In each test, a weight of approximately 0.25 g of sample was used. Nitrogen physisorption was performed at its boiling temperature.

2.3. Temperature programmed reduction

H_2 TPR was carried out on unpromoted, Au promoted and Pt promoted catalysts using a Zeton-Altamira AMI-200 unit equipped with a thermal conductivity detector (TCD). Argon was used as the reference gas, and 10% H_2 (balance Argon) was flowed at 30 cm^3/min as the temperature was increased from 50 to 1100 °C (~850 °C for Pt/ceria catalysts) at a ramp rate of 10 °C/min to observe the temperature of ceria surface shell reduction. The amount of catalyst used was approximately 200 mg.

2.4. X-ray absorption near-edge spectroscopy

X-ray absorption near-edge spectroscopy (XANES) spectra were recorded near the Pt, Au, and Ce L_{III} edges at the National

Synchrotron Light Source located at Beamline X-18b at Brookhaven National Laboratory, Upton, New York, and details are reported in earlier work [3,7]. Smooth, self-supporting wafers were gently pressed and loaded into an in situ flow cell, and the treatment gas was directed right to the sample area. After the cell was purged for a long time with helium, to remove air, the samples were treated in situ with hydrogen. In the case of the Pt/ceria catalysts [4], ~23% H_2 was used, balance helium, at a total flow rate of 650 cm^3/min. For the Au/ceria catalysts [8], ~17% H_2 was used, balance helium, at a total flow rate of 360 cm^3/min. Scans were obtained in transmission mode at 50 °C intervals to explore the reduction of not only the Pt or Au promoter component, but also the surface reduction of ceria. To estimate the extent of reduction of ceria, linear combination XANES fits were carried out using Ce^{3+} and Ce^{4+} reference spectra. Details are reported elsewhere [4,8].

2.5. Diffuse reflectance Fourier transform infrared spectroscopy (DRIFTS)

A Nicolet Nexus 870 was used, equipped with a DTGS-TEC detector. A high pressure/high temperature chamber fitted with ZnSe windows was utilized as the WGS reactor for in situ reaction measurements. The gas lines leading to and from the reactor were heat traced, insulated with ceramic fiber tape, and further covered with general purpose insulating wrap. Scans were taken at a resolution of four to give a data spacing of 1.928 cm^{-1}. Typically, 128 scans were taken to improve the signal to noise ratio. The sample amount utilized was 33 mg.

Feed gases (UHP) were controlled by using Brooks 5850 series E mass flow controllers. Iron carbonyl traps consisting of lead oxide on alumina (Calsicat) were placed on the CO gas line. All gas lines were filtered with Supelco O_2/moisture traps. During a run, the catalyst was first activated at 300 °C in hydrogen and cooled to 240 °C. The only exception to this pretreatment was the unpromoted sample, which was reduced at 500 °C before cooling to 240 °C. This is because of the higher activation temperature required (see TPR profiles). Formates were generated by CO adsorption, where the total flow was approximately 140 cm^3/min and the gas composition was 2.7% CO, balance N_2. After the pseudo-stabilized formate was generated, the cell was purged and a 42.5% D_2 mixture (balance N_2) was introduced into the cell at a total flow rate of 234 cm^3/min. Decomposition and exchange of the formate as a function of loading and metal type was followed.

2.6. Testing in a fixed bed reactor

Steady state catalytic activity measurements were conducted in a fixed bed reactor consisting of a 0.5 in. stainless steel tube with an internal thermocouple. For the Pt/ceria catalysts, experiments were conducted using 33 mg of catalyst diluted to 0.4 g with silica. For the less active Au/ceria catalysts, 660 mg of catalyst was utilized. The catalyst bed was supported on a bed of quartz glass wool. A steam generator consisted of a downflow tube packed with quartz wool heated by a ceramic oven and equipped with an internal thermocouple. Water was added to the steam generator by a thin needle welded to a 1.6 mm line. A precision ISCO Model 500D syringe pump was used to feed the water. Conditions were chosen to mimic those of the low temperature shift reactor of a fuel processor, with the exception that CO_2 was not included in the tests. The total gas flow was approximately 240 cm^3/min, with a composition of 1.6% CO, 52.4% H_2O, 41.9% H_2 and 4.1% N_2. Catalysts were activated in hydrogen (100 cm^3/min at 300 °C) prior to reaction testing.

3. Results and discussion

Table 1 provides the results of nitrogen physisorption. The BET surface areas were very similar for the catalysts studied, a necessary first step for comparing the impact of metal type and loading of the promoter. Temperature programmed reduction profiles are provided in Fig. 1 and have been reported elsewhere [4,8]. Reduction of ceria catalysts is a complicated process. In the simplest description, there are two main steps—ceria surface shell reduction at lower temperature and bulk reduction at higher temperature. For unpromoted ceria, these two steps occur at approximately 500 °C and close to 850 °C, respectively. However, when a metal promoter is loaded, the surface shell reduction is facilitated [1–4]. On a similar loading basis, Au promotes the reduction of the ceria surface shell to a lower temperature than that of Pt [8]. There are other important factors in the surface shell reduction process. Initially, charged ceria catalysts are covered by carbonate species. The metal promoter facilitates removal of a fraction of the carbonates during surface shell reduction, as evidenced by DRIFTS and TGA-MS experiments [4]. Furthermore, reduction of the surface shell is accompanied by the formation of Type II bridging OH groups on the surface. These are either formed via removal of surface capping oxygen atoms and subsequent dissociation of H_2O (Eq. (1)) [5] or by H_2 dissociation on the metal promoter, with spillover to the ceria surface (Eq. (2)) [4]. Intense identifying bands for Type II bridging OH groups are observed by infrared spectroscopy at ca. 3650 cm^{-1}. Their formation is facilitated in the presence of a metal promoter [4,8]. It is

Table 1
BET surface area and porosity measurements from physisorption of N_2 at 77 K

Sample name	BET SA (m^2/g)	Pore volume (cm^3/g)	Average pore radius (nm)
Pt series			
Unpromoted ceria	125	0.091	1.45
0.5% Pt/ceria	117	0.084	1.53
2.5% Pt/ceria	114	0.089	1.57
Au series			
Unpromoted ceria	121	0.087	1.43
0.5% Au/ceria	118	0.085	1.43
2.5% Au/ceria	116	0.085	1.47

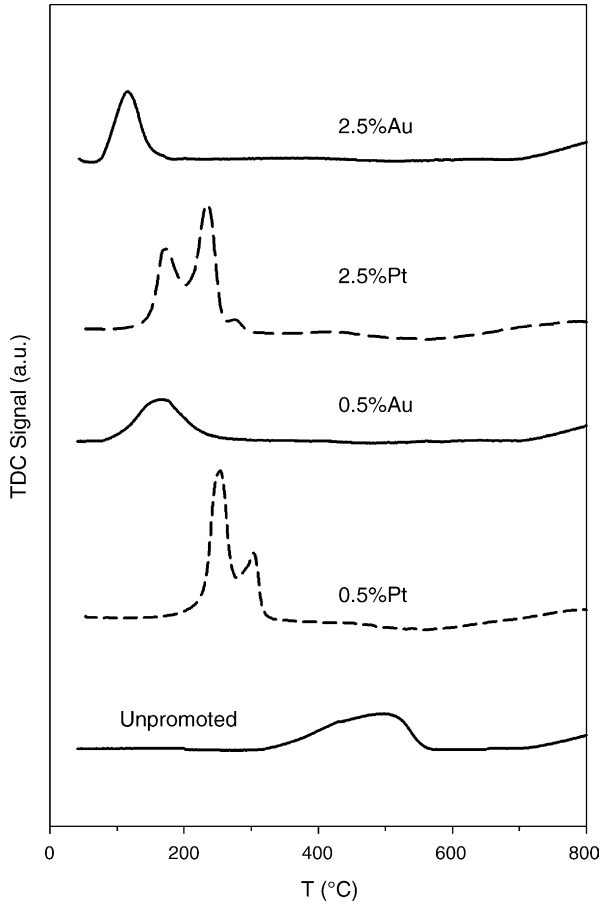

Fig. 1. TPR profiles of, moving upward: (a) unpromoted ceria; (b) 0.5% Pt/ceria; (c) 0.5% Au/ceria; (d) 2.5% Pt/ceria; and (e) 2.5% Au/ceria.

equally important to consider that the Type II bridging OH groups are associated with Ce^{3+} defect sites in the surface shell of ceria and can be interpreted to be H_2O dissociated at a vacancy.

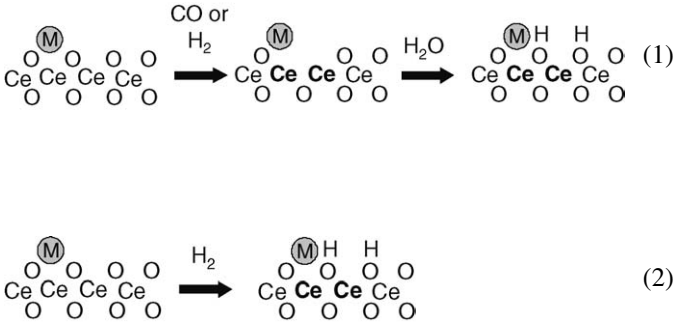

Therefore, quantifying the extent of reduction of ceria, as we have carried out using XANES (see Table 2), allows one to gain insight into the temperature at which these OH groups are formed, as well as indirectly their density [4]. We have observed in previous work that the metal promoter is initially present as an oxide. The promoter is first reduced, prior to the reduction of the ceria surface shell, which is why we currently favor a H_2 dissociation and spillover mechanism for the formation of the bridging OH groups [4,8]. The XANES results for Au and Pt promoters showed that the Au oxide reduced at a lower temperature than of Pt [8], and the ceria surface shell reduction was complete at a lower temperature for the Au promoted catalysts than for the Pt promoted ones [4,8]. With increasing loading (applies to both promoters), the metal–oxide interaction is overcome at lower temperatures, such that the metal promoter is more easily reduced at higher loading [4,8]. Consequently, the ceria surface shell reduction is facilitated with increased loading as well. The maximum threshold for surface shell reduction appears to be close to 20–25% ceria in Ce^{3+} oxidation state [4,8]. This result is very close to the range reported by El Fallah et al. [3], who correlated this range to a virtually full reduced ceria surface. As shown in Table 2, reduction at 300 °C ensures that we have obtained this threshold for all the catalysts studied in this work. The only exception to this treatment condition was the unpromoted ceria sample, which was reduced at 500 °C, due to the higher temperature required for activation (Fig. 1).

The data in Table 3 show, however, that despite the comparable extents of reduction of the catalysts, and therefore comparable site densities of bridging OH groups, two interesting observations for the conversion of CO during WGS. First, increasing metal loading led to improved WGS activity. Secondly, as noted in the introduction, the Pt catalysts were found to be far more active than the Au catalysts [8], which were all far more active than unpromoted ceria.

Recently, we have tested the WGS mechanism four different ways, and in each study, we found that a surface formate mechanism best described the catalysis. One such mechanism is provided below, which was advanced by Shido and Iwasawa [5]:

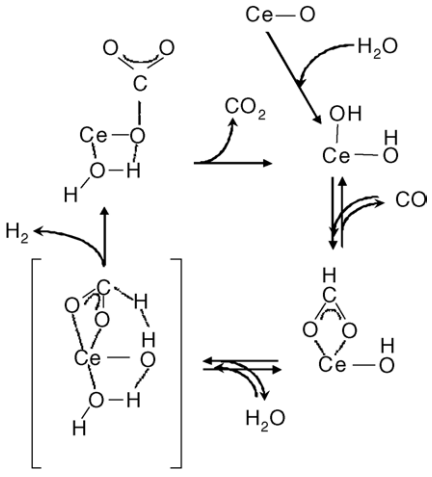

This mechanism is supported by four separate investigations, which will not be detailed in this study. Rather, we refer the reader to (1) dynamic formate coverage results [10,11], (2) steady state kinetic isotope effect studies [12], (3) transient kinetic isotope effect studies [13], and (4) results of isotope tracing [14]. As shown in the mechanism above, CO reacts with the Type II bridging OH groups to generate surface formate intermediates. Surface formates are quite

Table 2
Linear combination fits of XANES spectra with Ce^{3+} and Ce^{4+} reference compounds

T (°C)	No metal		0.5% Au		2.5% Au		0.5% Pt		2.5% Pt	
	Ce^{4+}	Ce^{3+}	Ce^{4+}	Ce^{3+}	Ce^{4+}	Ce^{3+}	Ce^{4+}	Ce^{3+}	Ce^{4+}	Ce^{3+}
50	100	0	99.2	0.8	99.5	0.5	98.9	1.1	99.1	0.9
100	–	–	97.9	2.1	98.7	1.3	97.8	2.2	97.1	2.9
150	–	–	86.8	13.2	79.1	20.9	–	–	–	–
200	–	–	78.7	21.3	76.5	23.5	96.5	3.5	89.3	10.7
250	–	–	77.0	23.0	75.1	24.9	92.5	7.5	77.9	22.1
300	97.0	3.0	74.7	25.3	75.2	24.8	76.0	24.0	75.9	24.1

Spectra recorded as a function of temperature in H_2 treatment.

stable at low temperatures, and decompose in inert gas flow in roughly 6–8 min at 300 °C for 1% Pt/ceria catalysts [13]. This process is primarily a reverse decomposition, back to CO and –OH [5,13]. However, when H_2O is introduced, formates decompose very rapidly and in the forward direction [5]. For example, they decompose in about 8 min at 140 °C [13]. The results are consistent with a reactant promoted formate decomposition, which is why Shido and Iwasawa included H_2O in the transition state of the forward decomposition [5]. We have confirmed rapid exchange of formate during ^{12}CO to ^{13}CO switching studies of the WGS reaction [14]. In inert gas flow, the formates were quite stable. Pt–CO exchanged rapidly whether or not the H_2O was included, indicating that the Pt–CO switch was probably only an exchange process [14].

In terms of a formate mechanism then the question is does the formate decomposition rate change during WGS as a function of the metal type and loading? We have noted that for Au catalysts, the steam-assisted formate decomposition was much slower relative to a similarly loaded Pt catalyst [8]. This suggests that the metal may be facilitating the C–H bond breaking of the formate, thereby promoting the rate limiting step. Note that the link between C–H bond breaking and the WGS rate is also strongly suggested by the kinetic isotope effect [5,12,13]. This not only is observed between switching from H_2O to D_2O during WGS, where the rate decreases by a factor of 1.4, but the same isotope effect is observed in the formate coverage response [5,12,13].

It is very difficult to assess the impact of the metal promoter on the formate decomposition when H_2O is present, since the formate decomposes so rapidly in the presence of steam [5,13]. Therefore, to isolate the promoting effect of the metallic function on the formate decomposition rate, we are examining in this work the thermal decomposition rate of the formate (i.e., reverse decomposition to CO and –OH) and the exchange rate from H-formate to D-formate in a D_2 flow. The question is, does the metallic function impact the C–H bond breaking rate of formate during reverse decomposition. If so, it should also promote C–H bond breaking during the forward shift.

Figs. 2–6 show the response of the formate during thermal decomposition in D_2. In the 3-D plots, labeled 'a', the H-formate decay is shown on the left (3060–2720 cm^{-1} region), while that of the D-formate formation (2230–2100 cm^{-1} region) is shown on the right. The decay of the formate (open circles) is calculated by summing up both the H- and D-formate contributions by area and dividing by the initial area. The fraction of formate exchanged (filled circles) is determined by dividing the area of the D-formate remaining to that of the sum of the H- and D-formates remaining. These plots are labeled 'b'.

As observed by comparing Figs. 2–6, there is a very interesting finding, that both the formate decay and exchange rates are heavily impacted by the presence/absence of metal, the metal type, as well as the loading. Just as in the trend of WGS activity, the Pt catalysts exhibit far greater activity for thermal formate decomposition than the Au catalysts [4,8], both of which are far more active than the unpromoted ceria catalyst. Secondly, increasing the promoter loading increases the formate decomposition rate [4,8]. A comparison of rates (based on the half-life) for both decomposition and exchange

Table 3
CO conversion during WGS in an atmospheric pressure fixed bed reactor using 3.75 cm^3/min CO:125 cm^3/min H_2O:100 cm^3/min H_2:10 cm^3/min N_2

Catalyst	Conversion of CO (mol%)							
	175 °C	200 °C	225 °C	250 °C	275 °C	300 °C	325 °C	350 °C
660 mg catalyst (GHSV: 21705 cm^3/h-gcat)								
Unpromoted ceria	0.8	1.0	1.5	2.1	3.2	6.2	–	–
0.5 wt.% Au	1.5	3.3	6.1	8.7	14.3	17.4	–	–
2.5 wt.% Au	8.1	13.7	22.7	34.3	52	58.3	–	–
33 mg catalyst (GHSV: 434090 cm^3/h-gcat)								
Unpromoted ceria	–	–	–	4.3	4.8	5.5	5.6	7.4
0.5 wt.% Pt	–	–	–	10.4	14.9	19.9	31.5	38.8
2.5 wt.% Pt	–	–	–	36.4	51.1	64.4	76.0	81.9

Note difference in space velocity (factor of 20).

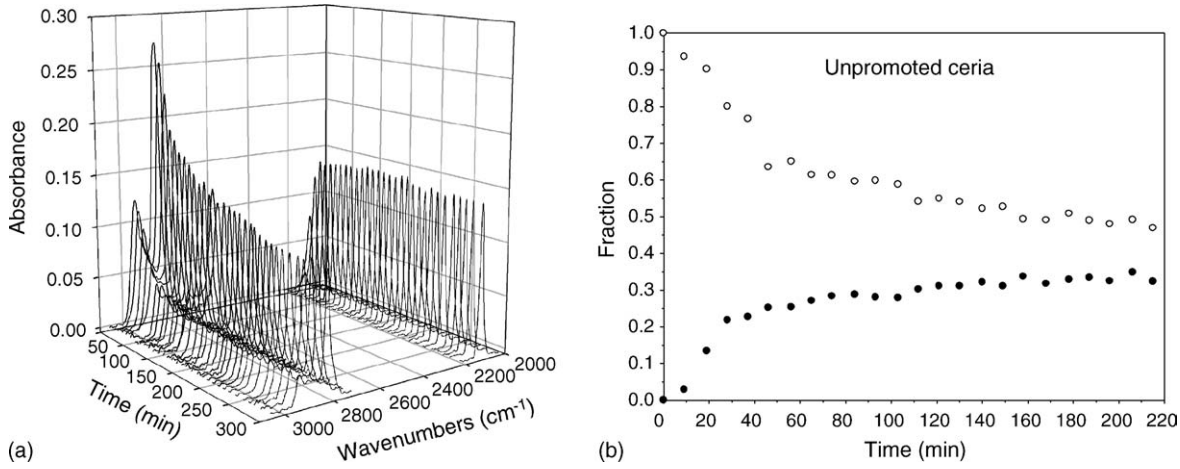

Fig. 2. (a) Unpromoted ceria (activated in H_2 at 500 °C)—response of the stabilized formate under deuterium (*conditions*: 33 mg catalyst, 240 °C, 42.5% D_2 mixture (balance N_2) at a total flow rate of 235 cm^3/min). (b) Unpromoted ceria (activated in H_2 at 500 °C)—response of the stabilized formate under deuterium (*conditions*: 33 mg catalyst, 240 °C, 42.5% D_2 mixture (balance N_2) at a total flow rate of 235 cm^3/min), including (open circles) decay of total formate {H + D} area signal and (filled circles) exchange of the formate {D/(H + D)}.

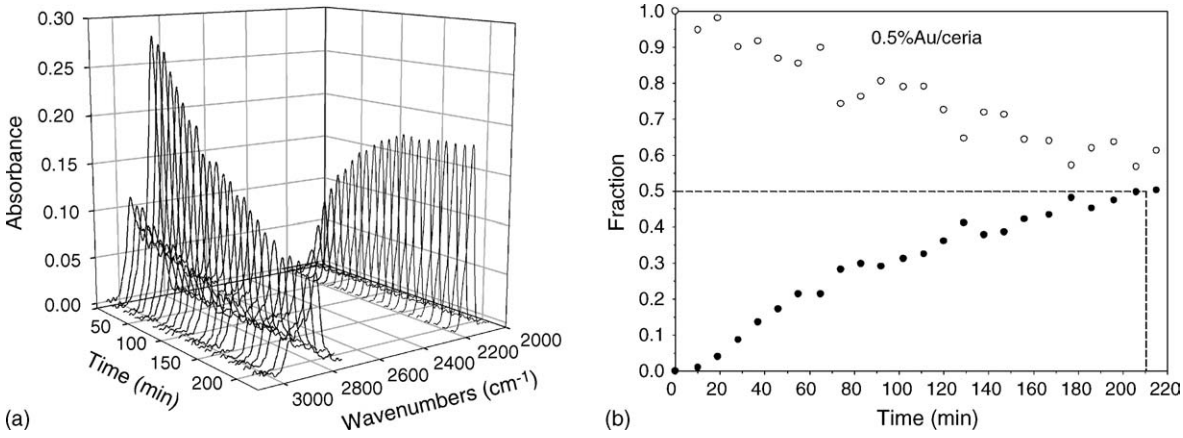

Fig. 3. (a) 0.5% Au/ceria (activated in H_2 at 300 °C)—response of the stabilized formate under deuterium (*conditions*: 33 mg catalyst, 240 °C, 42.5% D_2 mixture (balance N_2) at a total flow rate of 235 cm^3/min). (b) 0.5% Au/ceria (activated in H_2 at 300 °C)—response of the stabilized formate under deuterium (*conditions*: 33 mg catalyst, 240 °C, 42.5% D_2 mixture (balance N_2) at a total flow rate of 235 cm^3/min), including (open circles) decay of total formate {H + D} area signal and (filled circles) exchange of the formate {D/(H + D)}.

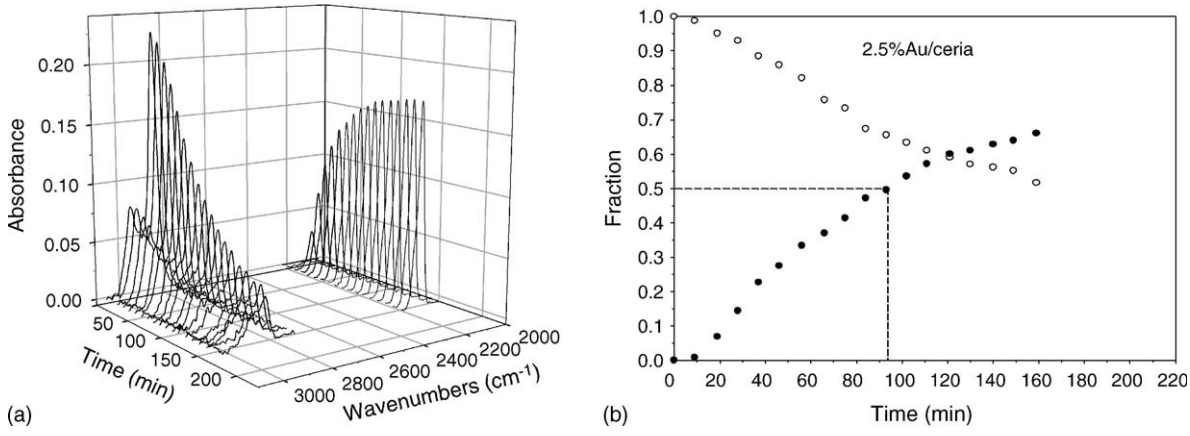

Fig. 4. (a) 2.5% Au/ceria (activated in H_2 at 300 °C)—response of the stabilized formate under deuterium (*conditions*: 33 mg catalyst, 240 °C, 42.5% D_2 mixture (balance N_2) at a total flow rate of 235 cm^3/min). (b) 2.5% Au/ceria (activated in H_2 at 300 °C)—response of the stabilized formate under deuterium (*conditions*: 33 mg catalyst, 240 °C, 42.5% D_2 mixture (balance N_2) at a total flow rate of 235 cm^3/min), including (open circles) decay of total formate {H + D} area signal and (filled circles) exchange of the formate {D/(H + D)}.

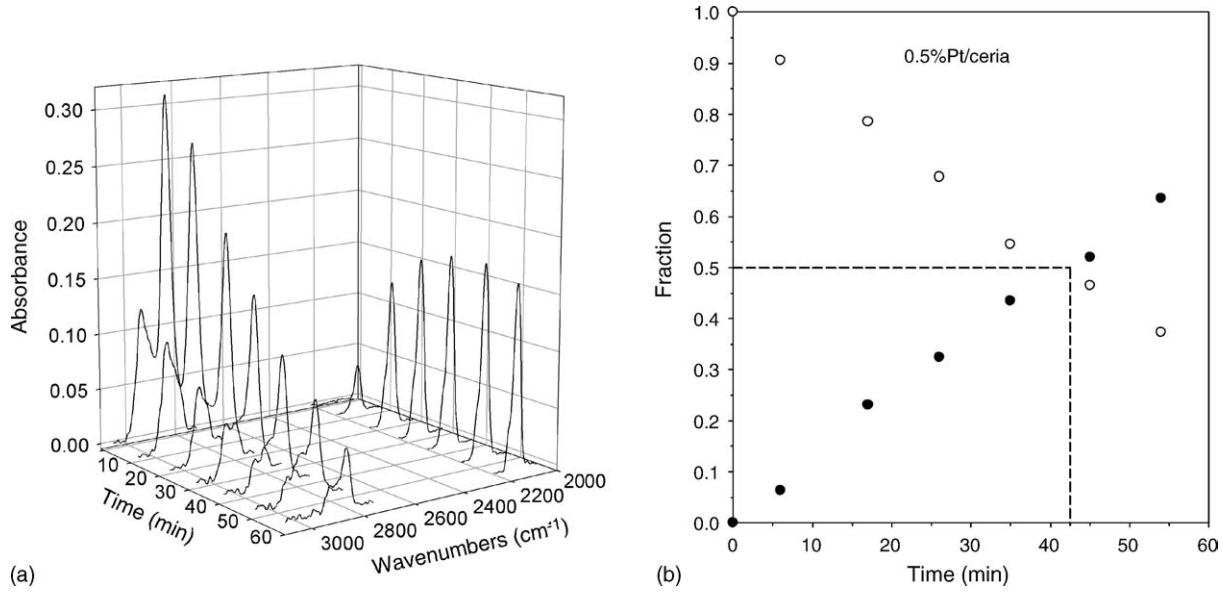

Fig. 5. (a) 0.5% Pt/ceria (activated in H_2 at 300 °C)—response of the stabilized formate under deuterium (*conditions*: 33 mg catalyst, 240 °C, 42.5% D_2 mixture (balance N_2) at a total flow rate of 235 cm^3/min). (b) 0.5% Pt/ceria (activated in H_2 at 300 °C)—response of the stabilized formate under deuterium (*conditions*: 33 mg catalyst, 240 °C, 42.5% D_2 mixture (balance N_2) at a total flow rate of 235 cm^3/min), including (open circles) decay of total formate {H + D} area signal and (filled circles) exchange of the formate {D/(H + D)}.

are tabulated in Table 4. The kinetic parameters are referenced to the 0.5% Au/ceria catalyst. The unpromoted ceria sample is not included, as it was activated at much higher temperature, and the exchange was so slow, that the sample did not achieve 50% exchange to the D-formate within the course of the experiment.

The method appears to provide an important way of ranking promoters, as the thermal formate decomposition rate provides a way to isolate the promoting effect of the metal from that of H_2O. From the WGS rates, both appear at this time to be very important for impacting the forward decomposition of the formate (see transition state) during WGS. The metal therefore likely provides a conduit for H_2 removal during WGS. This is not surprising, since the metallic function typically is utilized for hydrogenation/dehydrogenation reactions. Interestingly, Au is often studied for its lack of hydrogenation ability. That is, it is an important metal of study for partial hydrogenation reactions, like acetylene to ethylene [18], or butadiene to butene [19,20].

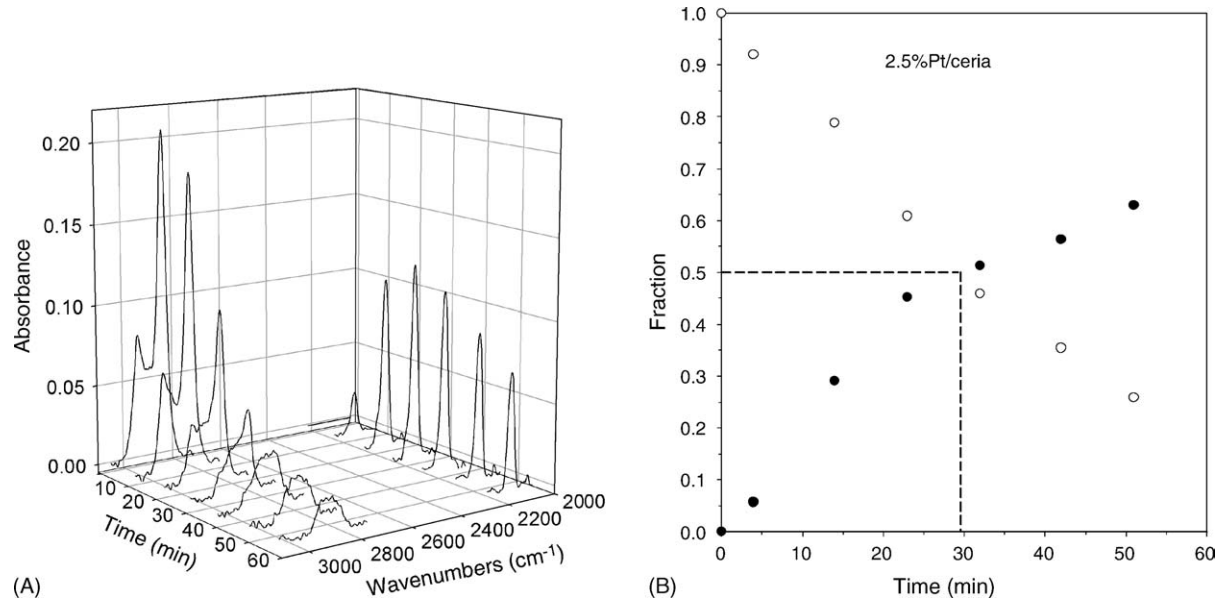

Fig. 6. (a) 2.5% Pt/ceria (activated in H_2 at 300 °C)—response of the stabilized formate under deuterium (*conditions*: 33 mg catalyst, 240 °C, 42.5% D_2 mixture (balance N_2) at a total flow rate of 235 cm^3/min). (b) 2.5% Pt/ceria (activated in H_2 at 300 °C)—response of the stabilized formate under deuterium (*conditions*: 33 mg catalyst, 240 °C, 42.5% D_2 mixture (balance N_2) at a total flow rate of 235 cm^3/min), including (open circles) decay of total formate {H + D} area signal and (filled circles) exchange of the formate {D/(H + D)}.

Table 4
Rates of the total {H + D} formate decomposition and exchange {D/(H + D)}at 240 °C

Catalyst	$T_{1/2}$, decay	$T_{1/2}$, exchange	k, decay × 10^{-3} min^{-1}	k, exchange × 10^{-3} min^{-1}	ΔE_A, decay relative to 0.5% Au/ceria (kJ/mol)	ΔE_A, exchange relative to 0.5% Au/ceria (kJ/mol)	Relative rates of exchange over decay
Ceria catalysts							
0.5% Au	272[a]	210	2.55	3.30	–	–	1.3
2.5% Au	163[b]	93	4.26	7.45	−2.2	−9.6	1.8
0.5% Pt	43	43	16.1	16.5	−7.9	−21.3	∼1.0
2.5% Pt	29	29	23.9	23.9	−9.5	−30.9	∼1.0

[a] Calculated from $C_A/C_{A0} = 0.6$ at $t = 200$ min.
[b] Calculated from $C_A/C_{A0} = 0.6$ at $t = 120$ min.

For those reactions, of course, Pt is far too active, leading to rapid full bond saturation. The results are also not surprising when one considers the history of the formate mechanism. The same catalysts that are good for WGS are those that are important for formic acid dehydrogenation. Since both reactions involve formate intermediates, the metallic function most likely assists in the dehydrogenation step.

The details of how the metal influences the catalysis have not been defined. If the metal only impacted the formate species near the boundary of the metal particle, only a small fraction of the surface formate would be converted and this is not the case. If, however, the formate surface species was mobile and its diffusion rate was rapid relative to the formate decomposition, the reaction could take place at or near the metal–ceria interface and still allow for decomposition of all of the surface formate species. In another view, the rate could be limited by H_2 formation and the metal provides a means to increase the rate due to a reverse spillover mechanism.

4. Conclusions

After ensuring that the extent of surface ceria shell reduction was similar among a series of metal/ceria catalyst, formates were generated by reaction of CO with the Type II bridging OH groups. Decomposition and exchange from H to D of the pseudo-stabilized formate was enhanced by switching from Au promoter to Pt. Likewise, increases in decomposition and exchange rates were observed by increasing the promoter loading from 0.5 to 2.5 wt.%. The results suggest that C–H bond breaking is facilitated during this thermal (reverse) decomposition to CO and –OH. Therefore, since the rate limiting step of the forward WGS reaction is strongly suggested, based on earlier kinetic isotope effect and isotopic tracer studies, to be associated with C–H bond breaking in the formate intermediate, the results could explain the enhancement in WGS rates observed by changing from Au to Pt and by increasing the loading.

Acknowledgments

The work was supported by the Commonwealth of Kentucky. We would like to thank Joel Young at the University of Oklahoma's Department of Physics for fabrication of the in situ X-ray spectroscopy cell. Research carried out (in part) at the NSLS, at BNL, is supported by the U.S. Department of Energy, Division of Materials Science and Division of Chemical Sciences, under Contract No. DE-AC02-98CH10886.

References

[1] H.C. Yao, Y.F.Y. Yao, J. Catal. 86 (1984) 254.
[2] Y. Li, Q. Fu, M. Flytzani-Stephanopoulos, Appl. Catal. B 27 (2000) 179.
[3] J. El Fallah, S. Boujana, H. Dexpert, A. Kiennemann, J. Marjerus, O. Touret, F. Villain, F. Le Normand, J. Phys. Chem. 98 (1994) 5522.
[4] G. Jacobs, U.M. Graham, E. Chenu, P.M. Patterson, A. Dozier, B.H. Davis, J. Catal. 229 (2005) 499.
[5] T. Shido, Y. Iwasawa, J. Catal. 141 (1993) 71.
[6] S. Hilaire, X. Wang, T. Luo, R.J. Gorte, J. Wagner, Appl. Catal. 215 (2001) 271.
[7] Q. Fu, A. Weber, M. Flytzani-Stephanopoulos, Catal. Lett. 77 (2001) 87.
[8] G. Jacobs, S. Ricote, P.M. Patterson, U.M. Graham, A. Dozier, S. Khalid, E. Rhodus, B.H. Davis, Appl. Catal. 292 (2005) 229.
[9] P. Mars, J.J.F. Scholten, P. Zwietering, Adv. Catal. 14 (1963) 35.
[10] G. Jacobs, L. Williams, U.M. Graham, D.E. Sparks, B.H. Davis, J. Phys. Chem. B 107 (2003) 10398.
[11] G. Jacobs, L. Williams, U.M. Graham, D.E. Sparks, B.H. Davis, Appl. Catal. A 252 (2003) 107.
[12] G. Jacobs, S. Khalid, P.M. Patterson, L. Williams, D.E. Sparks, B.H. Davis, Appl. Catal. 268 (2004) 255.
[13] G. Jacobs, P.M. Patterson, L. Williams, U.M. Graham, D.E. Sparks, B.H. Davis, Appl. Catal. 269 (2004) 63.
[14] G. Jacobs, A.C. Crawford, B.H. Davis, Catal. Lett. 100 (2005) 147.
[15] R.J. Gorte, S. Zhao, Catal. Today 104 (2005) 18.
[16] C. Binet, M. Daturi, J.C. Lavalley, Catal. Today 50 (1999) 207.
[17] G. Jacobs, A.C. Crawford, L. Williams, P.M. Patterson, B.H. Davis, Appl. Catal. 267 (2004) 27.
[18] T.V. Choudhary, C. Sivadinarayana, A.K. Datye, D. Kumar, D.W. Goodman, Catal. Lett. 86 (2003) 1.
[19] P.A. Sermon, G.C. Bond, J. Chem. Soc. Faraday Trans. I 74 (1978) 385.
[20] M. Okumura, T. Akita, M. Haruta, Catal. Today 74 (2002) 265.